A&A 444, 895–904 (2005)
DOI: 10.1051/0004-6361:20052782

Astronomy & Astrophysics

The qWR star HD 45166⋆,⋆⋆

I. Observations and system parameters

J. E. Steiner[1] and A. S. Oliveira[2,3]

[1] Instituto de Astronomia, Geofísica e Ciências Atmosféricas, Universidade de São Paulo, 05508-900, São Paulo, SP, Brasil
e-mail: steiner@astro.iag.usp.br
[2] SOAR Telescope, Casilla 603, La Serena, Chile
e-mail: aoliveira@ctio.noao.edu
[3] Laboratório Nacional de Astrofísica / MCT, CP21, Itajubá, MG, Brasil

Received 28 January 2005 / Accepted 3 July 2005

ABSTRACT

The binary star HD 45166 has been observed since 1922 but its orbital period has not yet been found. It is considered a peculiar Wolf-Rayet star, and its assigned classification has varied. For this reason we included the object as a candidate V Sge star and performed spectroscopy in order to search for its putative orbital period. High-resolution spectroscopic observations show that the spectrum, in emission and in absorption, is quite rich. The emission lines have great diversity of widths and profiles. The full widths at half maximum vary from 70 km s^{-1} for the weakest lines up to 370 km s^{-1} for the most intense ones. The hydrogen and helium lines are systematically broader than the CNO lines. Assuming that HD 45166 is a double-line spectroscopic binary, it presents an orbital period of $P = 1.596 \pm 0.003$ day, with an eccentricity of $e = 0.18 \pm 0.08$. In addition, a search for periodicity using standard techniques reveals that the emission lines present at least two other periods, of 5 and 15 h. The secondary star has a spectral type of B7 V and, therefore, should have a mass of about $M_2 = 4.8\ M_\odot$. Given the radial velocity amplitudes, we determined the mass of the hot (primary) star as $M_1 = 4.2 \pm 0.7\ M_\odot$ and the inclination angle of the system, $i = 0.77° \pm 0.09°$. As the eccentricity of the orbit is non zero, the Roche lobes increase and decrease as a function of the orbital phase. At periastron, the secondary star fills its Roche lobe. The distance to the star has been re-determined as $d = 1.3 \pm 0.2$ kpc and a color excess of $E(B-V) = 0.155 \pm 0.007$ has been derived. This implies an absolute B magnitude of −0.6 for the primary star and −0.7 for the B7 star. We suggest that the discrete absorption components (DACs) observed in the ultraviolet with a periodicity similar to the orbital period may be induced by periastron events.

Key words. techniques: spectroscopic – binaries: spectroscopic – stars: Wolf-Rayet

1. Introduction

HD 45166 has been observed since 1922 but its true nature remains a mystery. Anger (1933) described observations done between 1922 and 1933, showing that the emission spectrum is highly variable. The He II 4686 Å line is always present, with variable intensity, while the lines of N III 4640 Å and N IV 4058 Å appear and disappear completely. The star has been observed since, but no photometric or spectroscopic periodic variation has been discovered, in spite of the suspicion that it is, in fact, a binary system.

The spectral classification assigned to this object has varied with time. Anger (1933) proposed that the object is a Wolf-Rayet of the type WN. Neubauer & Aller (1948) classified it as a W7n. Morgan et al. (1955) classified it as Bpe while Hiltner & Schild (1968) returned to the WR classification. Hiltner (1956) described the object as having high excitation emission lines superposed upon an approximately O9 spectral type. Heap & Aller (1978), in a frequently cited (see for instance Willis & Stickland 1983 – WS83) but never published paper, classified the star as B8 V + qWR, that is, a binary with a B8 V component and a "quasi" Wolf-Rayet one. WS83 proposed a classification of B8 V + SdO – a main sequence star and a hot sub-dwarf. The Sixth Catalog of Galactic Wolf- Rayet Stars (van der Hucht et al. 1981) repeats for HD 45166 the classification proposed by Heap & Aller (1978) (B8 V + qWR) and puts it, together with V Sge, in the category of low mass WR, composed of only these two objects. This category does not exist in the Seventh Catalog of Galactic WR Stars (van der Hucht 2001), since neither HD 45166 nor V Sge are included in this catalog.

⋆ Based on observations made at the 1.5 m ESO telescope at La Silla, Chile, and at Laboratório Nacional de Astrofísica/CNPq, Brazil.
⋆⋆ Tables 2–5 are only available in electronic form at the CDS via anonymous ftp to cdsarc.u-strasbg.fr (130.79.128.5) or via http://cdsweb.u-strasbg.fr/cgi-bin/qcat?J/A+A/444/895

The star differs from a classic Population I WR in the sense that its emission lines are very narrow (typically full width at half maximum ($FWHM$) = 300 km s^{-1} for the He II lines). The object presents both characteristics of WN and WC simultaneously and seems to have a significant abundance of hydrogen judging from the He II Pickering decrement (Heap & Aller 1978; WS83). The object has a much smaller luminosity than a population I WR.

Van Blerkom (1978) made an analysis of the hydrogen and helium lines with the hypothesis that it is a population I WR object. He concluded that the WR component has a radius of 1 $R_\odot$ and has a small sized envelope that expands with a velocity of 150 km s^{-1}, which results in number densities of He II of about 10^{11} cm^{-3} and mimics the environment of a WR envelope. He found that the wind density is $N(\mathrm{H}) = 1.6 \times 10^{12}$ cm^{-3} and $N(\mathrm{He}) = 3.0 \times 10^{11}$ cm^{-3} and the mass loss rate, 4.5×10^{-8} $M_\odot$ year^{-1}. On the other hand, WS83 obtained, on the basis of ultraviolet observations with the IUE satellite, the following parameters for the WR component: $M_V = -0.21$; $T_{\rm eff} = 60\,000$ K; $\log(L/L_\odot) = 3.84$; $R = 0.77\ R_\odot$ and $M_1 = 0.5\ M_\odot$. They obtained, also, a distance of 1208 pc from spectroscopic parallax of the secondary star and a reddening of $E(B-V) = 0.15$ derived from the 2200 Å interstellar extinction band.

Willis et al. (1989) – WHSH89 – based on a sequence of high resolution IUE spectra, found constancy of the UV continuum, in contrast to the variability of the line spectrum. On long time scales they found variability in the intensities of the C IV, N IV, N V and He II emission lines. On short time scales, however, they found variability exclusively in the C IV 1559 Å doublet absorption lines. These short time scale variations (<1 day) are seen as discrete absorption components (DACs) characterized by two main features, with mean velocities of −950 km s^{-1} and −750 km s^{-1}. DACs are usually found in stars with P Cygni profiles. They can also be seen in luminous OB stars as well as in some SdO stars (see Brown et al. 2004 for a recent review on DACs). In HD 45166, both components are observed to migrate in velocity with an acceleration of ∼140 cm s^{-2}, a recurrence time of 1.60 ± 0.15 day and average lifetime of approximately 3 days. WHSH89 considered that these DACs in HD 45166 could result from structural changes in the wind, produced by radiative instabilities.

Until now photometric variability has not been detected in HD 45166. Ross (1961) carried out *UBV* observations on 24 nights and did not find any variation. WHSH89 performed 36 h of UV observations with the IUE satellite and did not find any variation with amplitude larger than 0.02 mag, that is, within the accuracy limit of the data. The photometric measurements published in the literature are summarized in Table 1.

There are several properties in common between HD 45166 and the V Sge stars: Van der Hucht et al. (1981) already compared the system to V Sge. With the parameters proposed by WS83 its mass ratio is inverted, as in the V Sge stars. Moreover, its emission line properties are quite similar. Therefore, we included HD 45166 in our ongoing search program for V Sge stars.

The V Sge stars are a group of 4 stars defined by Steiner & Diaz (1998): V Sge (Herbig et al. 1965; Diaz 1999), WX Cen (Oliveira & Steiner 2004; Diaz & Steiner 1995), V617 Sgr (Steiner et al. 1999; Cieslinski et al. 1999) and DI Cru (Oliveira et al. 2004; Veen et al. 2002). They are characterized by the presence of strong emission lines of O VI and N V. He II 4686 Å is at least two times more intense than Hβ. The V Sge stars are very similar to the Close Binary Supersoft X-rays Sources – CBSS – common in Magellanic Clouds, but not that frequent in the Galaxy. The CBSS are interpreted as binary systems with a white dwarf that presents hydrostatic hydrogen nuclear burning on its surface. This burning is due to the high mass transfer rate which is a consequence of the inverted mass ratio (see Kahabka & van den Heuvel 1997, for a review and references).

Table 1. Photometric magnitudes and colors from the literature.

Band	Measurement	Refs.
V	9.983; 9.88	1; 2
$B-V$	−0.064; −0.07	1; 2
$U-B$	−0.719; −0.76	1; 2
$V-R_{\rm C}$	0.072	1
$V-I_{\rm C}$	0.108	1
J	10.18; 9.81	3; 4
H	10.12; 9.75	3; 4
K	10.00; 9.57	3; 4

1– Menzies et al. (1990); 2– Hiltner (1956); 3– Ulla & Thejll (1998); 4– 2MASS all-sky survey.

The similarities between the spectra of HD 45166 and of the V Sge stars are the simultaneous presence of WN and WC characteristics, strong lines of hydrogen, as well as the ratios and widths of the emission lines. The main differences are that HD 45166 presents a spectrum of lower ionization: in spite of having N V, it does not show O VI. The star also has He I emission lines, unlike the V Sge or CBSS objects. On the other hand, unlike HD 45166, no V Sge star or CBSS has yet shown the spectrum of a secondary star.

In the next section we will describe our observations. In Sects. 3 and 4 we describe the optical spectrum of HD 45166 and the spectral classification of the secondary star. In Sect. 5 we derive the orbital period while in Sect. 6, two additional periods are proposed. In Sect. 7, the masses and orbital inclination are derived. In Sects. 8 and 9 we present the discussion and conclusions. In an accompanying paper (Paper II) we study the structure of the wind and discuss the nature of the system.

2. Observations

We obtained spectroscopic observations of HD 45166 from 1998 to 2004 (Table 2), using the Coudé spectrograph at the 1.6 m telescope of Laboratório Nacional de Astrofísica (LNA) in Itajubá, Brazil, and the Fiber-fed Extended Range Optical Spectrograph (FEROS) (Kaufer et al. 1999) at the 1.52 m telescope of the European Southern Observatory (ESO) in La Silla, Chile.

At the Coudé spectrograph we employed 600 l mm^{-1} and 1800 l mm^{-1} gratings, resulting in a spectral resolution of 0.7 and 0.2 Å $FWHM$ and reaching a S/N of about 20 to 30 at the continuum. We used a retro-illuminated Site (1024 × 1024)

CCD detector with 24 micrometer resolution elements. Several exposures of bias and flatfield were obtained to correct for the sensitivity of the CCD. Measurements of dark current were not necessary. The slit of the spectrograph was adjusted to 250 μm (about 1.1 arcsec). Observations of Thorium lamps were made for wavelength calibration. The data reduction was performed with the standard procedures, using IRAF[1] routines. Typical calibration rms residuals were of 2 mÅ for the 1800 l mm^{-1} grating observations.

The FEROS spectrograph, on the other hand, uses a bench-mounted echelle grating with reception fibers in the Cassegrain focus. Its measured spectral resolving power is $R = 48\,000$. A completely automatic online reduction system was used (Stahl et al. 1999). We obtained a total of 40 spectra with integration times of 15 min and readout time of about 7 min. The signal-to-noise ratio at the continuum for each individual spectrum was typically $S/N = 80$ at the central wavelength region (4500 through 7000 Å), decreasing to about $S/N = 35$ at the blue and red edges of the spectrum. The wavelength calibration rms residuals were of 7 mÅ. We cut the spectra in slices of 250 Å to normalize each slice by interactively fitting a low order Legendre polynomial to the continuum.

3. The optical spectrum

The average of the 40 spectra obtained with the FEROS spectrograph is presented in Fig. 1 in logarithmic scale. It presents a large set of lines in absorption as well as in emission (with a large number of telluric absorption lines). Quantitative characteristics of the lines are presented in Tables 3–5. The spectrum in absorption presents lines of H, He I, C II, N I, O I, Mg II, Si II and Fe II. Weak lines in absorption of C I, Mg I, Al II, Si I, P II, S II, Cr II, Fe I and Ni II are also present. The Fe II lines present an average heliocentric velocity of $V_r = +6.3 \pm 0.2$ km s^{-1}, where the uncertainty is the standard deviation divided by the square root of the number of measurements. This 0.2 km s^{-1} uncertainty is 30 times better than the spectral resolution. The lines of Si II have $V_r = +7.3 \pm 0.6$ km s^{-1} and the lines of O I, $V_r = +5 \pm 1$ km s^{-1}. He I lines have $V_r = +12 \pm 3$ km s^{-1}. The discrepancy between the radial velocities of He I lines and the other lines can be explained by the emission that can be seen in the blue wings of some of the He I lines as in the case of He I 4713 Å.

A complete list of absorption lines is given in Table 3 for all of the absorption lines with $W_\lambda > 0.02$ Å. Besides the measured wavelength we supply, also, the rest wavelength (in parenthesis), the radial velocity in the heliocentric system, the equivalent width, the *FWHM* and the identification of the species[2].

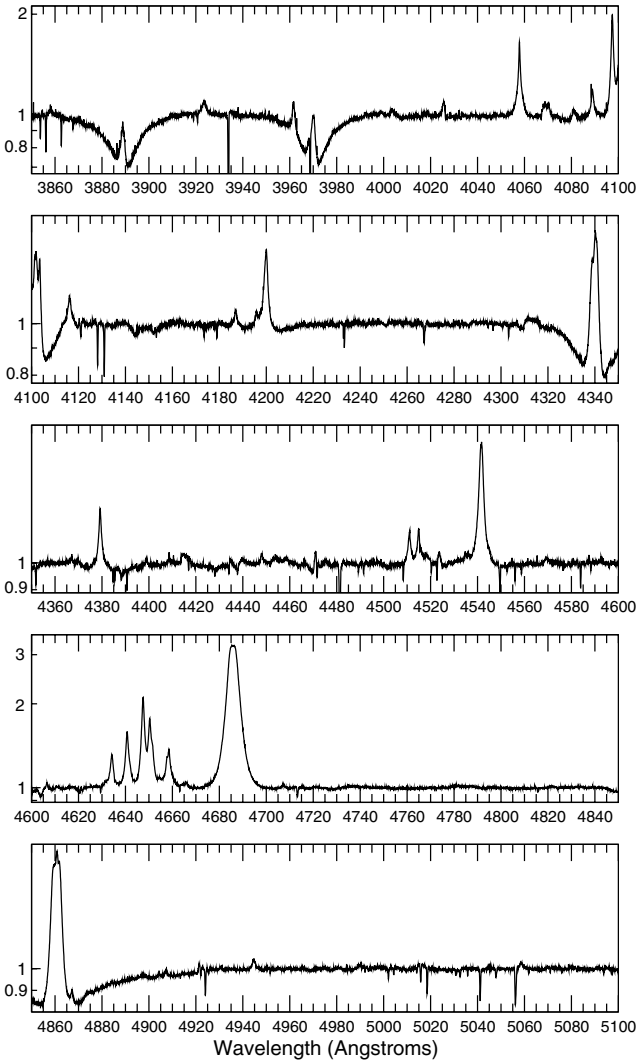

Fig. 1. Average normalized spectrum of HD 45166 obtained with the FEROS spectrograph. The ordinate is in logarithmic scale.

Isolated lines have radial velocities and widths that are comparable between them. Doublets, triplets and blended lines are easily identified by the discrepancies in the values of these measurements. Selected weak absorption lines are also shown in Table 4, where we present only species that are not listed in Table 3.

The emission spectrum is also quite rich, presenting lines of H, He I/II, C III/IV, N III/IV/V, O III and Si IV. In addition, it shows lines that are possibly O II and Si III, as well as some unidentified lines. The H lines are blended with lines of He II, and this affects the measurement of their widths and also their intensities. In Table 5 we show a list of all of the emission lines. We give the measured and rest wavelengths, the radial velocity in the heliocentric system, the equivalent width, *FWHM* and the identification of the species.

An important aspect of the emission line spectrum is the diversity of the widths and line profiles. The *FWHM* varies from 70 km s^{-1} for the weakest lines up to 370 km s^{-1} for the most intense ones. The H and He lines are systematically broader than the CNO lines and have a profile that can be described

[1] IRAF is distributed by the National Optical Astronomy Observatories, which are operated by the Association of Universities for Research in Astronomy, Inc., under cooperative agreement with the National Science Foundation.

[2] The line identifications were performed using the following online databases: the "NIST Atomic Spectra Database" (`http://www.physics.nist.gov/cgi-bin/AtData/main_asd`), the "Atomic Line List" (`http://www.pa.uky.edu/~peter/atomic/`) and the "Atomic Molecular and Optical Database Systems" (`http://amods.kaeri.re.kr/spect/SPECT.html`).

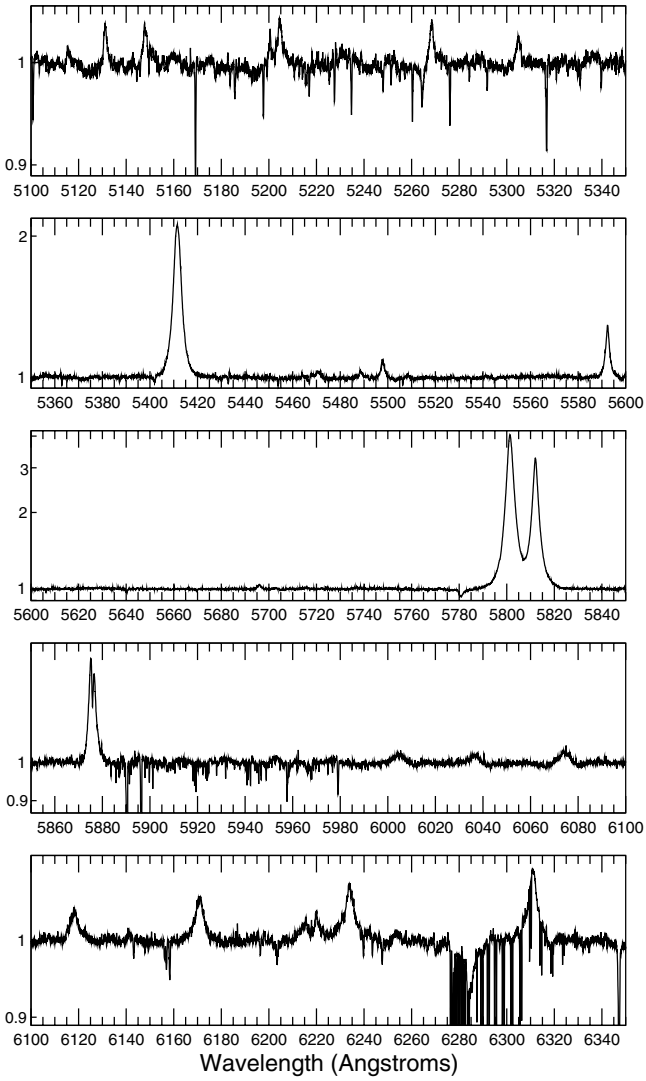

Fig. 1. continued.

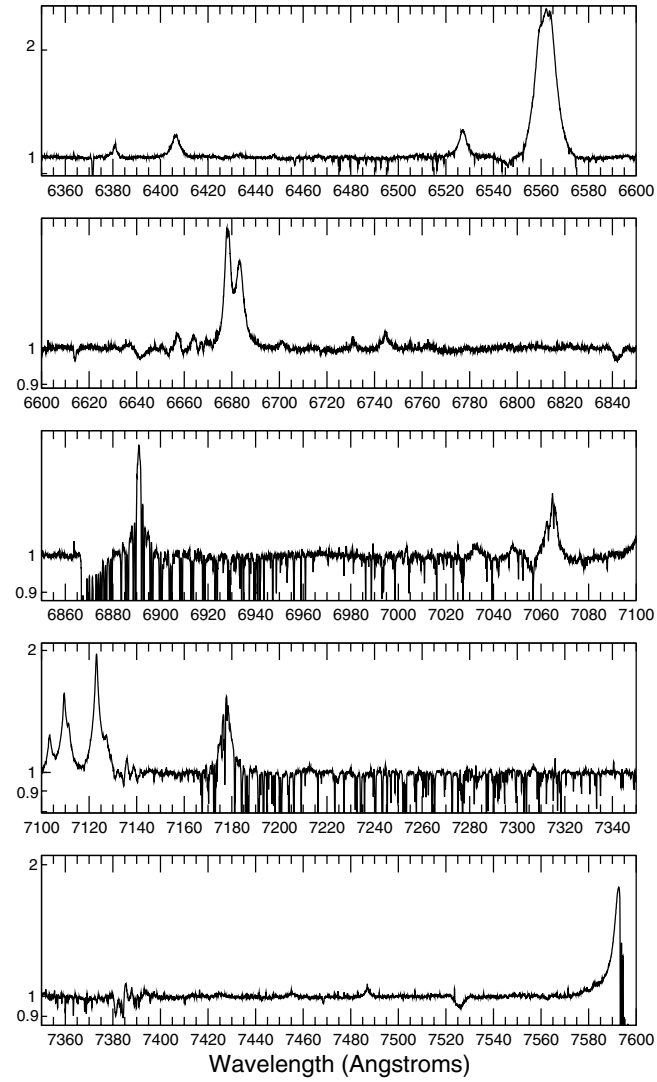

Fig. 1. continued.

approximately by a Voigt/Gauss profile, while the CNO lines are described by a Lorentz profile (see Fig. 2).

The emission line spectra observed in 1998, 1999, 2002 and 2004 are qualitatively similar. However, the equivalent width of the He II 4686 Å line decreased from 21.0 ± 0.5 Å in 1998 and 23.3 ± 0.4 Å in 1999 to 15.4 ± 0.4 Å in 2002, and increased again to 22.3 ± 0.5 Å in 2004. Still, the *FWHM* remained constant along these observations, conserving the value of 380 ± 10 km s^{-1}.

4. The spectral classification of the secondary star

The absorption spectrum of the secondary star was detected for the first time by Hiltner (1956) who described the spectrum of HD 45166 as of "high excitation superposed on a O9 type star". Heap & Aller (1978) classified the secondary as B8 V and this classification remains in use. With the high resolution and the high signal-to-noise ratio that characterize our data, we reassess the best classification for the star. Many of the conclusions, such as the values of the masses, depend critically on this parameter.

In order to re-evaluate the spectral class of the secondary component of the binary system, we compared the ratio of the observed Mg I 5183.6 Å/Mg II 4481.3 Å equivalent widths (W_λ(Mg I)/W_λ(Mg II) = 0.0464 ± 0.0038) to the ones given by the Kurucz (1994) models as provided by the VALD (Vienna Atomic Line Database) service (Kupka et al. 1999). We also compared this measured ratio to the ones found from the high resolution and high *S/N* ratio spectra of several B type stars from the UVES Paranal Observatory Project (Bagnulo et al. 2003). From both comparisons we derived a B7 ± 1 V spectral type. This classification is similar, within the errors, to that (B8 V) obtained by Heap & Aller (1978). According to Cox (1999), the properties of a B7V star are $T_{\rm eff}$ = 13 500 K, M = 4.8 $M_\odot$, R = 3.4 $R_\odot$ and M_B = −0.7.

5. The orbital period

Heap & Aller (1978) determined that HD 45166 is a binary system composed of a "quasi Wolf-Rayet" star and a B8 V star. With the observations described in the previous section, we may now verify whether this star has a detectable orbital

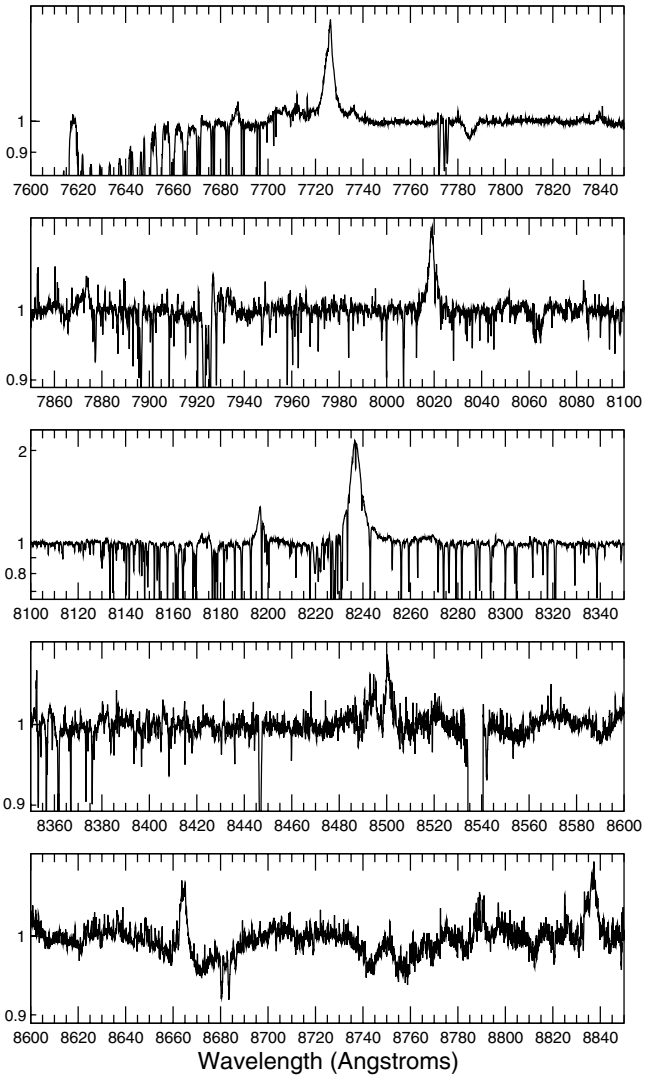

Fig. 1. continued.

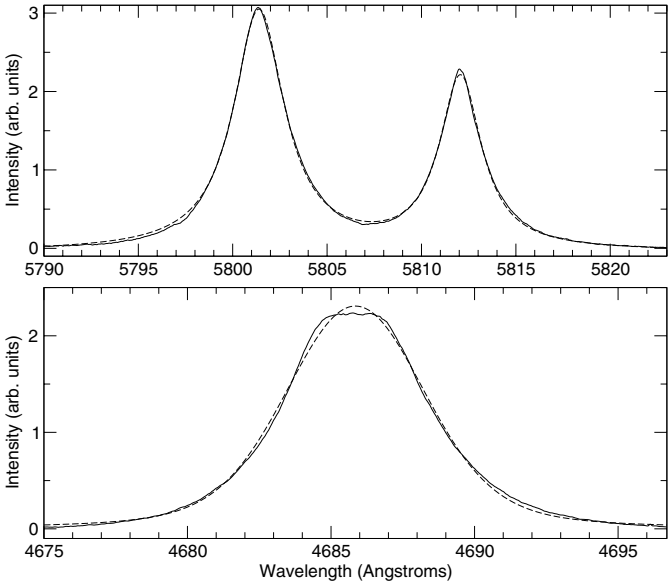

Fig. 2. *Top*: C IV 5801/11 Å emission lines (continuous line) and Lorentz profiles fitting (dashed line). *Bottom*: He II 4686 Å emission line (continuous line) and the Voigt profile fitting (dashed line).

period. If our data show radial velocity variations on both the emission and absorption features then we may be dealing with a double spectroscopic binary. However, previous observations revealed no radial velocity variability in excess of 10 km s^{-1} (WHSH89). Therefore it is very important that any measurement be made with maximum accuracy.

Photospheric absorption lines of a star are excellent tracers of its movement and potential indicators of an orbital period. To reach the necessary accuracy, we measured the radial velocities of the O I 7772/4/5 and 8446 Å absorption lines from the FEROS spectra and calculated their weighted average, taking as weight the equivalent widths, respectively $W_\lambda = 0.115$ Å (7772 Å), $W_\lambda = 0.133$ Å (7774 Å), $W_\lambda = 0.120$ Å (7775 Å) and $W_\lambda = 0.163$ Å (8446 Å). To proceed, we corrected the O I average radial velocities for possible uncertainties in the wavelength calibration. This correction was based on the averaged residuals of the nearby 7670.26 Å and 7671.31 Å telluric line observed wavelengths, as compared to their rest wavelengths. The use of telluric absorption lines as a stationary comparison source was analyzed by Griffin & Griffin (1973). In our case, to estimate the uncertainties resulting from this correction, the radial velocities of these two telluric lines differ by 0.2 km s^{-1} for the same exposure and by 0.5 km s^{-1} for different observations from the same night. Therefore, the uncertainty in the measurements of the O I lines position relative to the nearby telluric features may also be 0.2 km s^{-1}, even though the observed spectral line resolution in this region is 6.2 km s^{-1}. The relative dispersion of the radial velocities of O I in Fig. 4 (top diagram) suggests that this is quite reasonable. One could expect that measurements of absorption lines other than O I would have uncertainties of 0.5 km s^{-1}, because of the absence of such correction by close telluric features.

The CLEAN (Roberts et al. 1987) and PDM (Phase Dispersion Minimization, Stellingwerf 1978) routines for period searches applied to the O I average radial velocities indicate a period of $P = 1.596 \pm 0.003$ day (Fig. 3). The associated radial velocity curve (Fig. 4, top) has an amplitude of $K_2 = 2.4 \pm 0.2$ km s^{-1} and an eccentricity of $e = 0.18 \pm 0.08$. These parameters were obtained by fitting the data with the Russell-Wilsing (Binnendijk 1960) method.

The mass function is

$$f(M_1) = \frac{M_1^3 \sin^3 i}{(M_1 + M_2)^2} = \left(1.04 \times 10^{-7}\right)\left(1-e^2\right)^{3/2} K_2^3 P\,(M_\odot) \quad (1)$$

where K_2 is measured in km s^{-1} and P in day. With the values derived above we obtain a mass function of $f(M_1) = 2.2 \times 10^{-6}\ M_\odot$.

6. The 5 and 15 h periods

Since the emission spectrum (associated with the primary component of the binary system) is quite rich, we measured radial displacements of these lines to verify if the orbital period determined above is also seen in this component. In a first attempt (Oliveira & Steiner 2002) analyzing only the emission lines

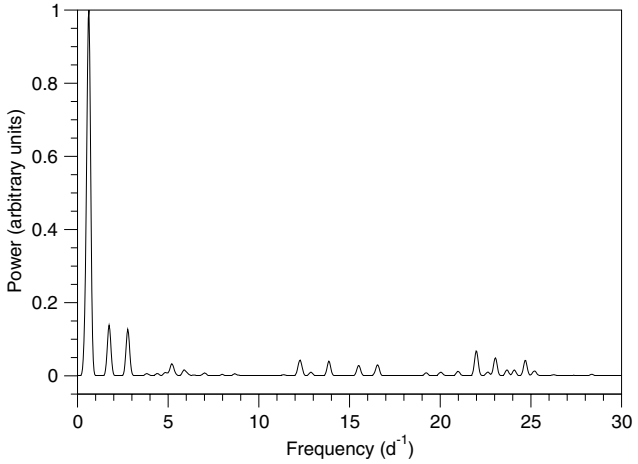

Fig. 3. The CLEAN periodogram for the O I average radial velocities shows a strong peak at frequency $f = 0.627$ d^{-1}, or $P = 1.596$ d.

from the data obtained at LNA in 1999, we found a candidate period of 0.357 day.

To measure the radial velocities of the emission lines from the FEROS spectra we used the C IV 5801/11 Å lines, because these features are narrower than the H and He lines and they are very well fitted by Lorentzian profiles (Fig. 2, top diagram). Also, they are located only 100 Å away from the Na I 5890/96 Å interstellar absorption lines (Fig. 5), which can be used as fiducial marks to correct for radial velocity inaccuracies. This is the same procedure we applied to the O I absorption lines above, when the fiducial references were telluric features. Therefore, the C IV radial velocity measurements were performed by simultaneously fitting Lorentz profiles and obtaining the simple average of both radial velocities. Then we subtracted, from this average, the residuals of the radial velocities of the Na I interstellar lines relative to their median value.

The resultant radial velocity curve shows a period of 0.205 day (5 h) (Fig. 6, top). The fact that two spectroscopic periods exist is a complicating factor because, with the small amplitudes involved, it is very difficult to determine them. Another factor that complicates the determination of the periods is that their values coincide with unit fractions of a day. We have confused (Oliveira & Steiner 2002) the period of 0.205 day ($\sim 1/5$ of a day) with 0.357 day ($\sim 1/3$ of a day). In the periodogram obtained from the LNA data, the most visible period is $\sim 1/3$ of a day. One should mention that the orbital period is $\sim 3/2$ of a day.

Which of the two periods we found is the orbital period? We believe that the 1.596 day period is orbital for two reasons. First, it was derived using the photospheric absorption lines from the secondary star. Second, the 5 h period is so short that, if it were orbital, the secondary star would not fit in its Roche lobe.

If the 1.596 ± 0.003 day period is the orbital one, we should find this period also in the primary star, that is, we should search for this period in the emission lines. To do this, we subtracted the average radial velocity curve, folded with the 5 h period, from the raw data of C IV radial velocity. The result is plotted as a function of the 1.596 day period (Fig. 4, bottom) and shows a curve symmetric to the absorption radial velocity curve with the same period, but with an amplitude slightly larger, that is, $K_1 = 2.7 \pm 0.2$ km s^{-1}. The radial velocity curve derived from the C IV emission lines is in anti-phase with the O I absorption lines curve. This should be expected if the emission and absorption lines are produced on distinct stellar components of the binary system and if the sample period is the orbital one. To investigate whether the C IV radial velocity variations could be attributed to superposed photospheric absorption features from the secondary component, we searched for C IV 5801/11 Å absorption lines in high resolution spectra of B stars. Our FEROS spectra of HD 103401 (B5 V), HD 104432 and HD 102465 (both B9 V), taken with the same instrumental configuration as the spectra of HD 45166, do not show any features above the noise that could be associated with C IV 5801/11 Å lines. This fact, together with the anti-phase behavior of the radial velocity curves, lead to the interpretation of the C IV radial velocity variations as produced by the orbital motion of the primary star.

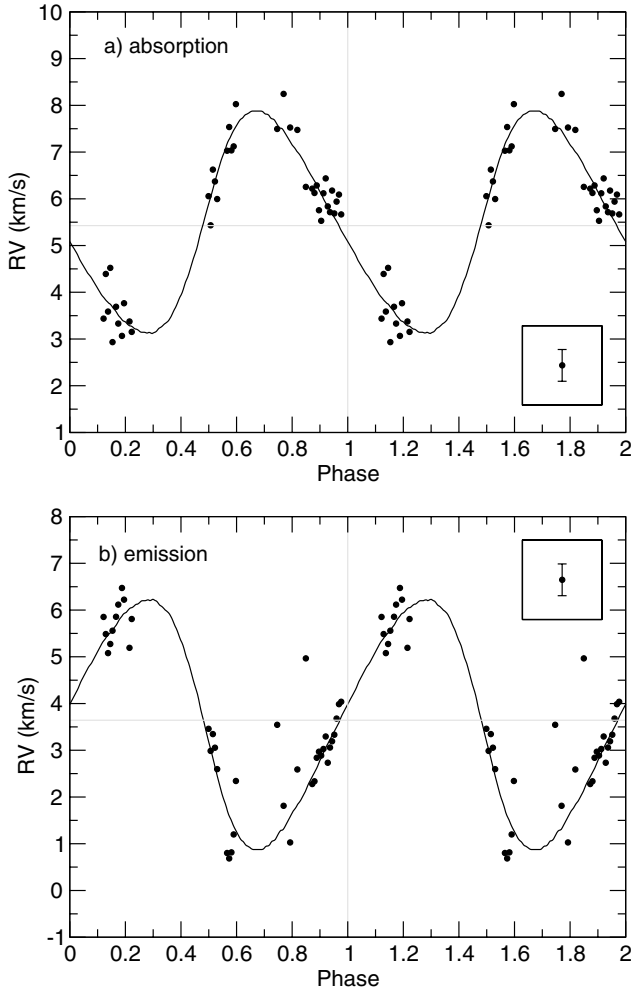

Fig. 4. Radial velocity curves for **a)** O I absorption lines, as a function of the orbital phase, folded to the 1.596 d period. **b)** C IV emission lines, as a function of the orbital phase, folded to the same 1.596 d period. The 5 and 15 h modulations (see Sect. 6) were subtracted from the latter. The inset show typical observational error bars.

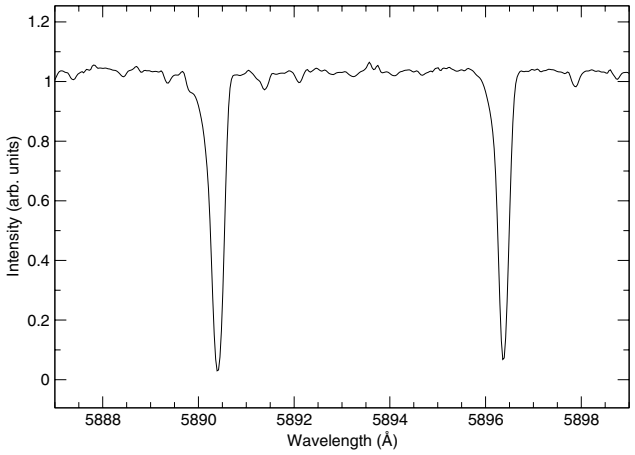

Fig. 5. The Na I interstellar absorption profiles, obtained with the FEROS spectrograph.

The mass function of the secondary component is

$$f(M_2) = 3.1 \times 10^{-6}\ M_\odot. \quad (2)$$

After we subtract the 1.596 day and the 5 h modulations, we applied the PDM routine on the residuals and we identified an additional period of 0.64 day (15 h, Fig. 6, bottom). Using these techniques, no other candidate period appeared with an amplitude greater than 0.5 km s^{-1}. In Paper II we will return to the non-orbital periods and their interpretation.

7. Masses and inclination

The orbital period was detected in both stars (associated with the absorption and also emission lines), so this system is a double spectroscopic binary. With the radial velocity amplitudes from both stars, we obtain

$$q = \frac{M_2}{M_1} = \frac{K_1}{K_2} = 1.13 \pm 0.11. \quad (3)$$

As a main sequence B7 V star, the mass of the secondary is $M_2 = 4.8 \pm 0.5\ M_\odot$; therefore $M_1 = 4.2 \pm 0.7\ M_\odot$. The mass of the primary star was estimated by WS83. They assumed that the primary star obeys the wind relations of typical OB stars. From an approximate wind model and observed P-Cygni profile parameters from IUE, they estimate a mass of 0.5 $M_\odot$. In that case the mass was not inferred from dynamical parameters such as radial velocity curves.

The inclination angle of the system, obtained from the mass function, is $i = 0.77° \pm 0.09°$. This is probably one of the smallest orbital inclination angles known for a binary system.

The major semi-axes of the orbits, (a_1, a_2), are defined as

$$a_{1,2}\ \sin\ i = \left(1.98 \times 10^{-2}\right)\left(1 - e^2\right)^{1/2} K_{1,2}\ P\ R_\odot \quad (4)$$

and, in the case of HD 45166, are $a_1 = 6.3 \pm 0.6\ R_\odot$ and $a_2 = 5.5 \pm 0.5\ R_\odot$.

Does the secondary star fill its Roche lobe? As the eccentricity of the orbit is non zero, the Roche lobes increase and decrease as a function of the orbital phase. At periastron, the

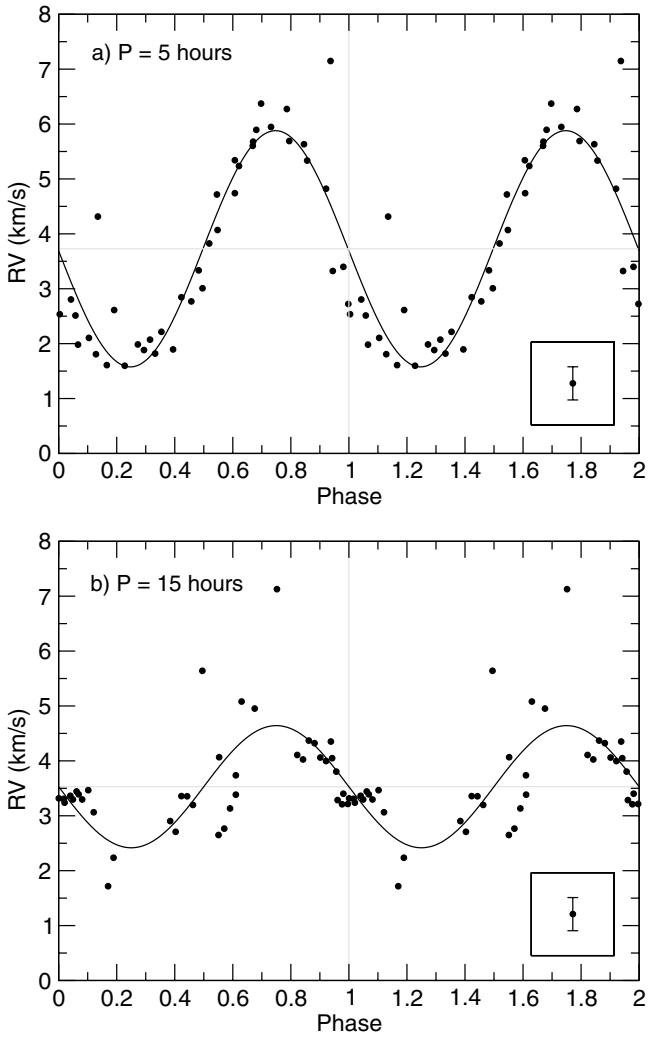

Fig. 6. Radial velocity curves for the C IV emission lines, as a function of **a)** the 5 h period (the 1.596 day and 15 h modulations were previously subtracted) and **b)** the 15 h period (the 1.596 day and 5 h modulations were previously subtracted). The inset show typical observational error bars.

Roche lobes have minimum dimensions and, at that phase, the effective radius of the secondary's lobe is given by (Hilditch 2001)

$$R_{r2}(\mathrm{min}) = \frac{4.21 P^{2/3}(1-e)(K_1+K_2)(0.38+0.20\log(M_2/M_1))M_1}{K_2(M_1+M_2)^{2/3}}\ R_\odot. \quad (5)$$

For the values determined for HD 45166, we have $R_{r2}(\mathrm{min}) = 3.7\ \pm 0.8\ R_\odot$. Considering the uncertainties, this value is very close to the secondary's radius (see Sect. 4) and, therefore, at periastron the secondary star may fill its Roche lobe.

The maximum radius for the secondary's Roche lobe is (Hilditch 2001)

$$R_{r2}(\mathrm{max}) = \frac{4.21\ P^{2/3}(1+e)(K_1+K_2)(0.38+0.20\ \log(M_2/M_1))M_1}{K_2(M_1+M_2)^{2/3}}\ R_\odot \quad (6)$$

Table 6. Basic parameters of the binary system.

Parameters of the system	
$P_{\rm orb}$ = 1.596 ± 0.003 day	e = 0.18 ± 0.08
T_0(HJD)= 2 452 097.03 ± 0.17	i = 0.77° ± 0.09°
K_2(abs) = 2.4 ± 0.2 km s^{-1}	K_1(emiss) = 2.7 ± 0.2 km s^{-1}
γ(HC) = +4.5 ± 0.2 km s^{-1}	ω = + 283° ± 28°
d = 1.3 ± 0.2 kpc	$E(B-V)$ = 0.155 ± 0.007
$q = M_2/M_1$ = 1.13 ± 0.11	
Parameters of the primary star	
P_1 = 0.205 day	M_1 = 4.2 ± 0.7$M_\odot$
K(0.205 d) = 2.3 ± 0.3 km s^{-1}	M_B = −0.6
T_1(HJD) = 2 452 299.62 ± 0.01	a_1 = 6.3 ± 0.6 $R_\odot$
P_2 = 0.64 day	
K(0.64 d) = 1.1 ± 0.4 km s^{-1}	
T_2(HJD) = 2 452 097.40 ± 0.06	
Parameters of the secondary star	
M_2 = 4.8 ± 0.5 $M_\odot$	a_2 = 5.5 ± 0.5 $R_\odot$
R_2 = 3.4 $R_\odot$	log g = 4.05
$T_{\rm eff2}$ = 13 500 K	Spectral type = B7±1 V
R_{r2}(min) = 3.7 ± 0.8 $R_\odot$	R_{r2}(max) = 5.4 ± 1.1 $R_\odot$
M_B = −0.7	

that is, 5.4 ± 1.1 $R_\odot$. In Table 6 we list the basic parameters for the system.

8. Discussion

8.1. Gravitational redshift

The General Theory of Relativity predicts the existence of gravitational redshift given by (for $z = v/c \ll 1$, where z is the redshift, v is velocity and c is the velocity of light)

$$z = \frac{V_{\rm gr}}{c} = \frac{GM}{R\,c^2} = \frac{2.11\times10^{-6} M/M_\odot}{R/R_\odot}. \quad (7)$$

At the surface of the secondary star this corresponds to $V_{\rm gr}$ = +0.9 km s^{-1} and for the primary star, $V_{\rm gr}$ = +2.0 km s^{-1} (where we considered R_1 = 1.3 $R_\odot$, see Paper II). As these values are larger than the precision of our measurements, they need to be taken into account in the data analysis. If the average velocity of the secondary absorption spectrum is +6.2 ± 0.3 km s^{-1}, then the expected average photospheric velocity in our spectra of the primary star should be of +7.3 km s^{-1}. The average heliocentric velocity of the secondary star, corrected for the gravitational redshift, is $\langle v(HC)\rangle$ = +5.3 ± 0.3 km s^{-1}. This velocity is not the radial velocity of the center of mass, because this depends on the sampling of the observation phases. The value of γ, that is, of the radial velocity of the mass center, is determined from the radial velocity curve and corresponds to the value that divides the curve in two segments of same underlying areas. Its value, obtained from the secondary star's absorption lines radial velocities and corrected for the gravitational redshift, is γ = 4.5 ± 0.2 km s^{-1} (Table 6).

8.2. The distance to the system

Heap & Aller (1978), as well as WS83 determined the distance to the system based on the secondary star spectroscopic parallax. The first authors found a distance of 1.26 kpc. They also determined that the neighboring star HD 44498 has a reddening of $E(B-V)$ = 0.14. WS83 determined a distance of 1.208 kpc. The color excess measured by them is $E(B-V)$ = 0.15 and it is quite reliable, given that it is based on the interstellar extinction band at 2200 Å.

In order to obtain an independent estimate of the interstellar extinction, we measured the equivalent width of the diffuse interstellar band (DIB) at 5780 Å and found W_λ(5780 Å) = 100 ± 6 mÅ. Using the relation of the DIB equivalent width versus $E(B-V)$ color excess (Somerville 1988)

$$E(B-V) = [W_\lambda(5780\ \text{Å}) + 46]/940 \quad (8)$$

where W_λ is given in mÅ, we obtain, $E(B-V) = 0.155 \pm 0.007$. The estimated error does not take into account the uncertainty of Somerville's calibration. The two methods of estimating the color excess agree quite well. However, the DIB at 5780 Å may be contaminated by the N IV 5776.3 Å emission line.

We measured the equivalent width of Mg II 4481 Å from the FEROS spectra of two comparison stars and obtained for HD 103401 (B5 V), W_λ(4481 Å) = 0.263 ± 0.005 Å and for HD 102465 (B9 V), W_λ(4481 Å) = 0.377 ± 0.004 Å.

Interpolating the spectral type one would expect, for the B7 ± 1 V secondary component of HD 45166, $W_\lambda(4481\ \text{Å}) = 0.320 \pm 0.005$ Å. We found 0.177 ± 0.005 Å, instead, due to the dilution from the companion's continuum. This means that the secondary star contributes 55% ±2% in the B filter, and the distance to HD 45166 is, therefore, $d = 1.3 \pm 0.2$ kpc.

The radial velocity of the interstellar Na I lines determined by us (see Table 3) is 22.8 km s^{-1} in the heliocentric system. After correcting this value to the Local Standard of Rest (LSR) we obtain a radial velocity of $V_{\rm LSR} = +7.1$ km s^{-1}. From the galactic rotation curve we obtain, for the coordinates of HD 45166 ($l = 203.1°/b = -2.3°$), the expected radial velocity of 10.8 (d/kpc) km s^{-1}. The radial velocity of the average stellar spectrum, corrected for the gravitational redshift, is $V_{\rm LSR} = -9.0$ km s^{-1}. We conclude, therefore, that the star has an anomalous velocity of approximately −23.1 km s^{-1} with respect to LSR.

8.3. DACs and the photospheric connection

The coincidence between the orbital period ($P = 1.596 \pm 0.003$ day) and the recurrence time of 1.60 ± 0.15 day (WHSH89) for the Discrete Absorption Components (DACs) is striking. Why should there be an association between the recurrent appearance of slowly accelerating clouds and the orbital period? The clouds responsible for the periodic absorption seem to be ejected at each orbit. What could be the periodic event responsible for this ejection? The non-zero eccentricity may play a key role in this. At each orbit there is a periastron event in which the secondary fills its Roche lobe and is capable of transferring matter to the primary. This periodic accretion may be physically related to the DACs but how, exactly, is not clear at this point. We will revisit this issue in Paper II.

9. Conclusions

In what follows we present the main conclusions of this paper:

1. The optical spectrum of HD 45166 presents a great wealth of information both in the emission as well as in the absorption spectrum. The emission spectrum has lines of H, He I/II, C III/IV, N III/IV/V, O II/III/IV, Si III/IV. The spectrum in absorption has lines of H, He I, C II, N I, O I, Si II, Mg II and Fe II. Weak lines of C I, Mg I, Si I, P II, S II, Cr II and Fe I are also seen.
2. We classified the spectral type of the secondary star as B7 V and, therefore, it should have a mass of $M_2 = 4.8\ M_\odot$ and a radius of $R_2 = 3.4\ R_\odot$.
3. The emission lines have a great diversity of widths and profiles. The most intense lines have a *FWHM* of 370 km s^{-1} and the weakest lines of 70 km s^{-1}. Lines of H and He have Voigt/Gauss profiles and are systematically broader than the lines of CNO, that have Lorentz profiles.
4. HD 45166 is shown to be a double spectroscopic binary with orbital period of 1.596 ± 0.003 day and eccentricity of $e = 0.18 \pm 0.08$.
5. Standard techniques for period search applied to the emission lines show two additional periods, of 5 and 15 h.
6. The amplitude of the radial velocities of the orbital period are $K_1 = 2.7 \pm 0.2$ km s^{-1} and $K_2 = 2.4 \pm 0.2$ km s^{-1}. We derived $M_1 = 4.2 \pm 0.7\ M_\odot$ and $i = 0.77° \pm 0.09°$.
7. The secondary star's radius may be about the size of its Roche lobe at periastron. Therefore we can consider that, at periastron, it fills or it is very close to filling its Roche lobe.
8. The expected gravitational redshift is 0.9 km s^{-1} for the secondary star and 2.0 km s^{-1} for the primary. These values are larger than the precision of our measurements and they need to be taken into account in the analysis of the data.
9. We estimated to HD 45166 a color excess of $E(B-V) = 0.155 \pm 0.007$ and a distance of 1.3 ± 0.2 kpc.
10. We suggest that the discrete absorption components (DACs) observed in the ultraviolet with a periodicity similar to the orbital period may be induced by the periastron events.

Acknowledgements. We would like to thank Dr. Albert Bruch for his careful reading of the manuscript and the anonymous referee for the constructive comments. We are specially grateful to Dr. Luiz Paulo Vaz for kindly fitting the measurements of the radial velocity with his program of orbit adjustment with non-zero eccentricity. A. Oliveira thanks FAPESP for financial support.

References

Anger, C. 1933, Bull. Harvard Coll. Obs., 891
Bagnulo, S., Jehin, E., Ledoux, C., et al. 2003, Messenger, 114, 10
Binnendijk, L. 1960, in Properties of Double Stars, 163
Brown, J. C., Barrett, R. K., Oskinova, L. M., et al. 2004, A&A, 413, 959
Cieslinski, D., Diaz, M. P., & Steiner, J. E. 1999, AJ, 117, 534
Cox, A. N. 1999, in Allen's Astrophysical Quantities, ed. Cox, Los Alamos, NM Fourth Edition (AIP Press)
Diaz, M. P. 1999, PASP, 111, 76
Diaz, M. P., & Steiner, J. E. 1995, AJ, 110, 1816
Griffin, R., & Griffin, R. 1973, MNRAS, 162, 243
Hilditch, R. W. 2001, in An Introduction to Close Binary Stars (Cambridge: Cambridge University Press)
Heap, S. R., & Aller, L. H. 1978, unpublished
Herbig, G. H., Preston, G. W., Smak, J., & Paczynski, B. 1965, ApJ, 141, 617
Hiltner, W. A. 1956, ApJS, 2, 389
Hiltner, W. A., & Schild, R. E. 1968, ApJ, 143, 770
Kahabka, P., & van den Heuvel, E. P. J. 1997, ARA&A, 35, 69
Kaufer, A., Stahl, O., Tubbesing, S., et al. 1999, Messenger, 95, 8
Kupka, F., Piskunov, N. E., Ryabchikova, T. A., Stempels, H. C., & Weiss, W. W. 1999, A&AS, 138, 119
Kurucz, R. L. 1994, SAO, Cambridge, CDROM 20-22
Menzies, J. W., Marang, F., & Westerhuys, J. E. 1990, SAAOC, 14, 33
Morgan, A. D., Code, A. D., & Whitford, A. E. 1955, ApJS, 2, 41
Neubauer, F. J., & Aller, L. H. 1948, ApJ, 107, 281
Oliveira, A. S., & Steiner, J. E. 2002, in the Physics of Cataclysmic Variables and Related Objects, ed. B. T. Gansicke, K. Beuermann, & K. Reinsch (ASP), ASP Conf. Ser., 261, 649
Oliveira, A. S., & Steiner, J. E. 2004, MNRAS, 351, 685

Oliveira, A. S., Steiner, J. E., & Diaz, M. P. 2004, PASP, 116, 311
Roberts, D. H., Lehar, J., & Dreher, J. W. 1987, AJ, 93, 968
Ross, L. W. 1961, PASP, 73, 354
Somerville, W. B. 1988, MNRAS, 234, 655
Stahl, O., Kaufer, A., & Tubbesing, S. 1999, in Optical and Infrared Spectroscopy of Circumstellar Matter, ed. E. W. Guenther, B. Stecklum, & S. Klose (ASP), ASP Conf. Ser., 188, 331
Steiner, J. E., & Diaz, M. P. 1998, PASP, 110, 276
Steiner, J. E., Cieslinski, D., Jablonski, F. J., & Williams, R. E. 1999, A&A, 351, 1021
Stellingwerf, R. F. 1978, ApJ, 224, 953
Ulla, A., & Tejll, P. 1998, A&AS, 132, 1
Van Blerkom, D. 1978, ApJ, 225, 175
Van der Hucht, K. A. 2001, New Astr. Rev., 45, 135
Van der Hucht, K. A., Conti, P. S., Lundstrom, I., & Stenholm, B. 1981, Space Sci. Rev., 28, 227
Veen, P. M., van Genderen, A. M., & van der Hucht, K. A. 2002, A&A, 385, 619
Willis, A. J., & Stickland, D. J. 1983, MNRAS, 203, 619 (WS83)
Willis, A. J., Howarth, I. D., Stickland, D. J., & Heap, S. R. 1989, ApJ, 347, 413 (WHSH89)